# NMR Studies of Retinoid-Protein Interactions: The Conformation of [$^{13}$C]-β-Ionones Bound to β-Lactoglobulin B

**Robert W. Curley, Jr.,[1,3] Appavu K. Sundaram,[1] John W. Fowble,[1] Frits Abildgaard,[2] William M. Westler,[2] and John L. Markley[2]**

*Received December 30, 1998; accepted January 30, 1999*

***Purpose.*** Vitamin A (retinol) and its metabolites comprise the natural retinoids. While the biological action of these molecules are thought to be primarily mediated by ca. 55 kDa nuclear retinoic acid receptors, a number of structurally similar 15-20 kDa proteins are involved in the transport, and possibly metabolism, of these compounds. The milk protein β-lactoglobulin B (β-LG) is an 18 kDa protein which binds retinol and may be involved in oral delivery of retinol to neonates. β-LG also binds drugs and other natural products and is of potential interest as a protective delivery vehicle.

***Methods.*** To examine the conformation of the model retinoid β-ionone both in solution and when bound to β-LG, NMR and computational methods have been employed.

***Results.*** Taken together, NMR studies of β-ionone in solution measuring scalar and dipolar coupling, as well as CHARMm calculations, suggest β-ionone prefers a slightly twisted 6-s-*cis* conformation. Isotope-edited NMR studies of $^{13}$C-labeled β-ionones bound to β-LG, primarily employing the HMQC-NOE experiment, suggest β-ionone also binds to β-LG in its 6-s-*cis* conformation.

***Conclusions.*** The methods employed here allow estimates of protein-bound ligand conformation. However, additional sites of ligand labeling will be necessary to aid in binding site localization.

**KEY WORDS:** $^{13}$C-edited; NMR; retinol; retinoic acid; β-lactoglobulin.

## INTRODUCTION

Retinoic acid (**1**; Fig. 1) is a metabolite of retinol (**2**) which performs the functions of the vitamin in maintaining growth and epithelial tissue differentiation in mammals. As a result, **2** and its analogues (retinoids) have been developed to treat dermatologic diseases and are being studied as cancer chemopreventive/chemotherapeutic agents (1). The actions of the water-insoluble, labile polyene **1** are mediated through association with a number of transport and receptor proteins. At physiological concentrations, **2** binds to the ~21 kD serum retinol-binding protein (SRBP) and is transported in the plasma to target tissues (2). The structure of this protein shares remarkable similarity to a number of other hydrophobic ligand-binding globular proteins as well as to the ~16 kD cellular retinol-binding protein (CRBP) and cellular retinoic acid-binding protein (CRABP) which may serve to regulate intracellular retinoid metabolism and/or retinoid delivery to the nucleus (3). Most recently, a family of ~55 kD nuclear retinoic acid receptors have been discovered that resemble the family of steroid hormone receptors and likely mediate retinoid effects on differentiation by alterations in gene expression after ligand binding (4).

Since the actions of these molecules depend on the binding to a number of proteins, an interest in understanding the structure of these proteins both with and without bound ligand has developed. Structures of these proteins have most often been determined by X-ray diffraction. The secreted SRBP, as well as the more recently described extracellular epididymal retinoic acid-binding protein, forms a hydrophobic barrel composed of a series of twisted antiparallel β-sheets with their respective retinoid ligands bound in this hydrophobic pocket. In these cases the ligand trimethylcyclohexenyl ring is bound innermost in the barrel and the polar terminal group extends toward the protein surface. In contrast, X-ray structures of the cytosolic CRBP and CRBPII show remarkable similarity to the SRBP in their hydrophobic β-barrel motif but bind **2** with the terminal hydroxyl group innermost and the cyclohexenyl ring near the exterior of the binding pocket.

NMR spectroscopy has been less extensively used for studying the structure of these proteins or the conformation and localization of bound retinoid. Using cross-polarization magic angle spinning techniques, Griffin and co-workers have found that the visual pigment chromophore retinal (**3**) binds to opsin with an extended side chain and a 6-s-*trans* conformational relationship (see Fig. 1) between the cyclohexene ring and polyene chain (5). $^{19}$F-NMR Studies by Li and co-workers of 6-fluoro-tryptophan substituted CRBPs allowed the identification of tryptophan residues in the putative retinol-binding site via monitoring of $^{19}$F-shifts upon binding of **2** (6). Using $^{13}$C-labeled **1**, this same group has used NMR methods to suggest **1** binds to CRABPII in a twisted 6-s-cis relationship but that its conformation when bound to CRABPI is less clear (7). Earlier solution NMR and computational chemistry studies of uncomplexed ligands such as **3** and β-ionone (**4**) have led to the prediction of a preferred conformation for these molecules in which the planar extended side chain bears a slightly twisted 6-s-*cis* relationship to the cyclohexenyl ring (8,9) as opposed to the 6-s-*trans* conformation observed for bound ligand in the studies of opsin. These X-ray and NMR studies of retinoid binding proteins have recently been comprehensively reviewed (10).

The ~18 kD protein β-lactoglobulin B (β-LG) is one of the most abundant whey proteins is bovine milk and is found in the milk of many other mammalian species (11). While this protein has often been utilized as a model globular protein for biophysical studies, no definitive function has yet been assigned for the molecule. In recent years the protein has been found to

[1] Division of Medicinal Chemistry and Pharmacognosy, College of Pharmacy, The Ohio State University, Columbus, Ohio 43210.

[2] Department of Biochemistry and the NMR Facility at Madison, University of Wisconsin-Madison, Madison, Wisconsin 53706.

[3] To whom correspondence should be addressed. (e-mail: curley.1@osu.edu)

**ABBREVIATIONS:** SRBP, serum retinol-binding protein; CRBP, cellular retinol-binding protein; CRABP, cellular retinoic acid-binding protein; NMR, nuclear magnetic resonance; β-LG, β-lactoglobulin B; NOE, nuclear Overhauser enhancement; 2D, two-dimensional; HMQC, heteronuclear multiple quantum correlation; COSY, correlation spectroscopy; TOCSY, total correlation spectroscopy; GARP, globally optimized alternating-phase rectangular pulses; DIPSI, decoupling in the presence of scalar interactions.



0724-8741/99/0500-0651$16.00/0 

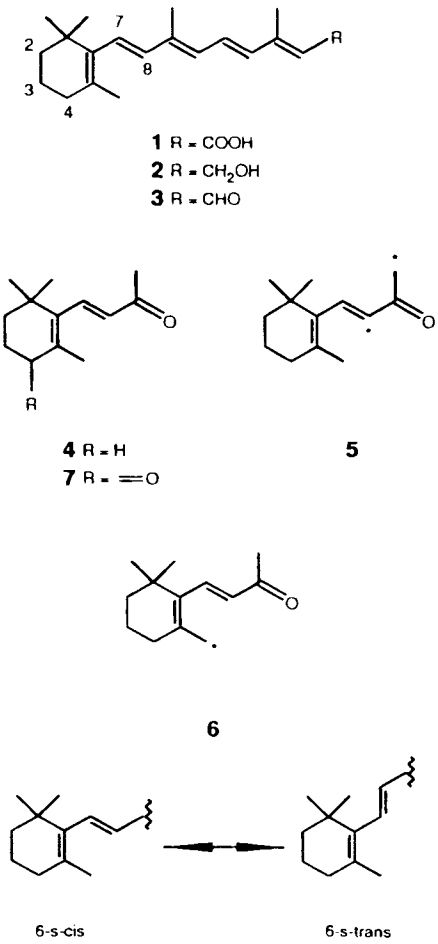


**Fig. 1.** Structures of retinoids.

bind a number of hydrophobic molecules, including drugs. In particular, fatty acids and **2** are found to bind to β-LG with good affinity (12). The stability of β-LG at low pH has led to the suggestion that the protein serves to bind and protect acid-labile ligands such as **2** and deliver them from maternal milk to the intestine of the suckling neonate. Evidence for putative intestinal receptors for the uptake of β-LG bound **2** has been presented (13), although others question whether this is an important function for β-LG (14). Nonetheless, β-LG does bind **2** with good affinity (Kd $\cong 2 \times 10^{-8}$ M) as well as the simpler retinoid **4** (Kd $\cong 6 \times 10^{-7}$ M) (15), and X-ray crystal analyses of β-LG have shown that it, too, bears remarkable structural similarity to the SRBP (16). The level of resolution of these crystal structures with regard to bound **2** has been modest and both the conformation and location of bound **2** remains unclear. Based on studies of ligand binding to β-LG, it has been proposed that there may be two distinct sites for **2**, one in the hydrophobic β-barrel and one in a surface hydrophobic cleft, even though **2** binds only with 1:1 stoichiometry to β-LG (17). Doubt has, however, also been cast on this concept (18,19). A number of questions remain with regard to the binding of **2** to β-LG and the abundance of this protein and its similarity to the SRBP make it a useful model for studying the conformation of protein-bound retinoid. In addition, the ability of β-LG to bind a number of small hydrophobic molecules has led to research on the use of the protein to protect and deliver labile ligands (15) which should be facilitated by a better understanding of ligand-β-LG interaction.

Isotope-edited NMR studies of stable isotope-labeled ligands have been developed to permit selective identification of the conformation of macromolecule-bound ligands and occasionally identify the characteristics of the ligand binding site (20). Here we describe our $^{13}$C-edited $^{1}$H-NMR studies of the conformation of two different versions of $^{13}$C-labeled **4** bound to β-LG and compare this with the preferred conformation of free retinoids as estimated by solution NMR and computational chemistry studies. In both of these environments we find retinoid assumes a twisted 6-s-*cis* conformation.

## MATERIALS AND METHODS

### Materials

Retinoic acid, β-cyclocitral, and β-lactoglobulin B were purchased from Sigma Chemical Co. Unlabeled β-ionone was from Aldrich Chemical Co. The [1,3-$^{13}C_2$]-acetone (99 atom %), $^{13}CH_3I$ (99 atom %) $D_2O$, $CD_3CD_2OD$, 85% $D_3PO_4$, and 40% NaOD employed in the studies were from Cambridge Isotope Laboratories (Andover, MA). $^{13}C_2$-Labeled β-ionone (**5**) was prepared by Aldol condensation of purified β-cyclocitral and [1,3-$^{13}C_2$]-acetone as previously described (21). $^{13}$C-Labeled β-ionone (**6**) was synthesized as outlined below. The 4-oxo-β-ionone (**7**) used in ligand NOE studies was also prepared as previously described (22). Fourier transformed NMR spectra were obtained on sample solutions in amber glass 175 × 5 mm sample tubes (Wilmad; Buena, NJ) to prevent photoisomerization.

### Preparation of $^{13}$C-β-ionone 6

The synthesis of [5-$^{13}CH_3$]-β-ionone (**6**) is summarized in Fig. 2. Briefly, the known key ketoester **8** was synthesized in good yield in two steps by the described procedure (23). Treatment of **8** with five equivalents of $^{13}CH_3MgI$ prepared *in situ* gave hydroxyester **9** after stirring 5 hours at reflux and 5 days at room temperature in ether (40% yield). Dehydration with $POCl_3$ in pyridine gave unsaturated ester **10** in 52% yield after chromatography and the ester was reduced ($LiAlH_4$, ether) to alcohol **11** in 65% yield. Oxidation of **11** to labeled β-cyclocitral **12** proceeded poorly using $MnO_2$. Attempts to achieve the same by Swern oxidation ($(COCl)_2$, DMSO, $Et_3N$) also failed. However, pyridinium chlorochromate oxidation of **11** gave purified **12** in 60% yield. Aldol condensation of **12** with acetone (21) gave **6** chromatographically and spectroscopically identical to **4**. Details of the preparation of these compounds are shown below.

### Synthesis of 2-carbomethoxy-3,3-dimethylcyclohexanone (8)

Two grams of this known compound were prepared by the published method (23) in 66% yield after column chromatography on silica gel using 5% ethyl acetate/hexane: $^{1}$H NMR ($CDCl_3$) δ 1.0 (s, 3,-$CCH_3$), 1.1 (s, 3,-$CCH_3$), 1.45 (m, 2, -$CCH_2$-(C-CO), 1.8 (m, 2, -$CH_2$C-C-CO), 2.2 (m, 1, -$CH_a(H_b)$-CO), 2.55 (m, 1, -$CH_b(H_a)$CO), 3.1 (s, 1,-CO-CH(C)-CO), 3.65 (s, 3, -$CO_2CH_3$).

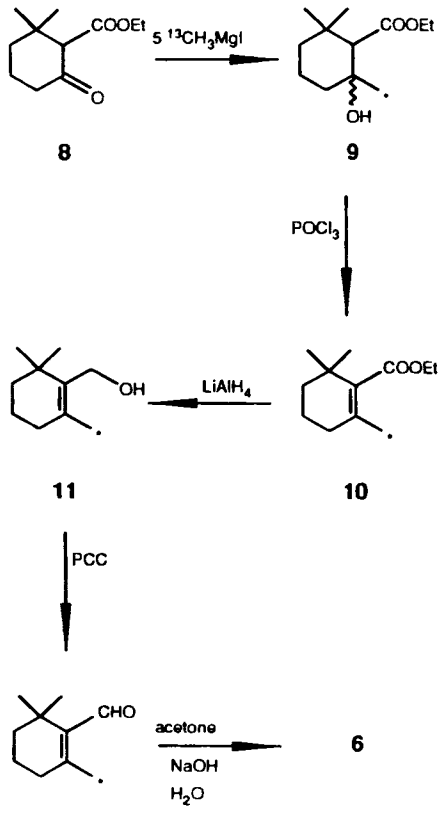


Fig. 2. Synthesis of [$^{13}$C]-**6**.

### Synthesis of [1-$^{13}CH_3$]-1,3,3-trimethyl-1-hydroxy-2-carbomethoxycyclohexane (9)

To a refluxing solution of 0.65 g of Mg in 150 mL of ether under Ar was added 3.8 g (27 mmol) of $^{13}CH_3I$. The mixture was refluxed for 1 hr before dropwise addition of 1 g (5.4 mmol) of **8** followed by 5 hr of reflux. The reaction mixture was then stirred at room temperature for 5 days. The mixture was then poured into 100 mL of water, 10 mL of acetic acid added, and extracted with 2 × 100 mL of ether. The combined ether layer was washed with water, saturated sodium bicarbonate, dried ($MgSO_4$) and solvent removed under reduced pressure to give crude **9**. Column chromatography on silica gel using 20% ethyl acetate/hexanes gave 436 mg (40%) of **9**. $^1$H NMR ($CDCl_3$) δ 1.02 (d, $J_{CH}$ = 126 Hz, 3, [1-$^{13}CH_3$]), 1.09 (s, 6, -$(CH_3)_2$), 1.4 (m, 2, 4-$CH_2$), 1.75 (m, 2, 5-$CH_2$), 1.9 (t, 2, 6-$CH_2$), 2.1 (s, 1, 2-CH), 3.72 (s, 3-$CO_2CH_3$); $^{13}$C NMR ($CDCl_3$) δ 31.0 (1-[$^{13}CH_3$]); HRMS *m/z* (%) 201.14469 ($M^+$, 2.21); calculated mass for $^{13}C_1C_{10}H_{20}O_3$ = 201.14466.

### Synthesis of [1-$^{13}CH_3$]-1,3,3-trimethyl-2-carbomethoxycyclohexene (10)

To 1.0 g (5 mmol) of **9** in 20 mL of pyridine was added 2 mL of $POCl_3$ dropwise at 0°C. The reaction mixture was stirred at room temperature for 14 hrs then diluted with 20 mL of petroleum ether and slowly quenched with 10 mL of water at 0°C, at a rate of 1 drop of water/minute. The aqueous layer was then extracted with 100 mL of petroleum ether and the organic layer washed with 20% HCl, saturated NaCl, dried ($MgSO_4$), and the solvent removed under reduced pressure to provide 606 mg (67%) of **10**: $^1$H NMR ($CDCl_3$) δ 1.0 (s, 6, -$(CH_3)_2$), 1.45–1.68 (m, 4, 4-$CH_2$, 5-$CH_2$), 1.65 (d, $J_{CH}$ = 126 Hz, 3, 1-[$^{13}CH_3$]), 2.0 (t, 2, 6-$CH_2$), 3.72 (s, 3, -$CO_2CH_3$); $^{13}$C NMR ($CDCl_3$) δ 19.6 (1-[$^{13}CH_3$]).

### Synthesis of [1-$^{13}CH_3$]-1,3,3-trimethyl-2-hydroxymethylcyclohexane (11)

To 1.0 g (5.5 mmol) of **10** in dry ether was added 420 mg (11 mmol) of $LiAlH_4$ and the mixture was stirred at room temperature for 4 hr. The reaction was quenched by adding 100 mL of water and the aqueous layer was extracted with 100 mL of ether. The combined ether layers were washed with saturated sodium chloride, dried ($MgSO_4$) and the solvent removed under reduced pressure. Compound **11** was obtained in 60% yield (507 mg) after column chromatography on silica gel eluting with 20% ethyl acetate/hexanes: $^1$H NMR ($CDCl_3$) δ 1.1 (s, 6, -$(CH_3)_2$), 1.42 (m, 2, 4-$CH_2$), 1.59 (m, 2, 5-$CH_2$), 1.71 (d, $J_{CH}$ = 126 Hz, 3, 1-[$^{13}CH_3$]), 1.98 (t, 2, 6-$CH_2$), 4.1 (s, 2, C-$CH_2$-O); $^{13}$C NMR ($CDCl_3$) δ 19.2 (1-[$^{13}CH_3$]).

### Synthesis of [5-$^{13}CH_3$]-β-cyclocitral (12)

To 200 mg (1.3 mmol) of **11** dissolved in 49 mL of $CH_2Cl_2$ and 1 mL of pyridine was added 500 mg of pyridinium chlorochromate. The mixture was stirred for 2 hr. and then 100 mL of dry ether was added and the supernatant decanted from a deposited black solid. The solid was washed with further dry ether, the combined ether portions were passed through a Florisil pad and the solvent removed under reduced pressure to give 140 mg (71%) of **12**: $^1$H NMR ($CDCl_3$) δ 1.09 (s, 6, -$(CH_3)_2$), 1.45 (m, 2, 2-$CH_2$), 1.61 (m, 2, 3-$CH_2$), 2.08 (d, $J_{CH}$ = 126 Hz, 3, 5-[$^{13}CH_3$]), 2.18 (t, 2, 4-$CH_2$), 10.1 (s, 1, -CHO); $^{13}$C NMR ($CDCl_3$) δ 21.8 (5-[$^{13}CH_3$]); GC (Supelco SPB-1 column, 100 to 175°C at 5°C/min) $t_R$ = 4.9 min (unlabeled β-cyclocitral, $t_R$ = 4.9 min).

### Synthesis of [5-$^{13}CH_3$]-β-ionone (6)

100 mg (0.65 mmol) of **12** was converted to **6** by the method described for preparing **5** (21) to give 70 mg (56%) of **6** (greater than 95 atom% $^{13}$C as determined by $^1$H NMR and mass spectrometry): UV (MeOH) $\lambda_{max}$ 293 nm (ε 11,100); $^1$H NMR ($CDCl_3$) δ 1.05 (s, 6, 1,1-$(CH_3)_2$), 1.4 (m, 2, 2-$CH_2$), 1.62 (m, 2, 3-$CH_2$), 1.71 (d, $J_{CH}$ = 126 Hz, 3, 5-[$^{13}CH_3$]), 2.05 (t, 2, 4-$CH_2$), 2.28 (s, 3, 10-$CH_3$), 6.09 (d, $J_{HH}$ = 16.2 Hz, 1, 8-CH), 7.22 (d, $J_{HH}$ = 16.2 Hz, 1, 7-CH); $^{13}$C NMR ($CDCl_3$) δ 22.2(5-[$^{13}CH_3$]); HRMS *m/e* (%) 193.15539 ($M^+$, 5.89); calculated mass for $^{13}C_1$ $C_{12}H_{20}O$ = 193.15486; GC (as for **12**) $t_R$ = 11.5 min (unlabelled β-ionone, $t_R$ = 11.5 min).

### Ligand NMR Studies

$^1$H NMR and nuclear Overhauser enhancement (NOE) difference experiments, performed at ambient temperature using deoxygenated solutions, were obtained on an IBM AC270 spectrometer operating at 270.13 MHz. Long range proton coupling constants were measured by high resolution analysis on a Bruker AM500 spectrometer at 500.13 MHz.

In typical NOE difference experiments a sufficient number of transients to ensure accurate integration were acquired using a sweep width of 2000–2500 Hz over 16K data points. Irradiations on resonances of interest, and one off-resonance control, were conducted cyclically in groups of eight scans preceded by 2–4 dummy scans. An irradiation time of 5 s, a pulse width of 2–4 μs (35–70°), and a low decoupling power (typically 60 dB attenuation of 200 mW channel) were used.

### Energy Calculations

Calculations and conformation predictions were conducted using QUANTA/CHARMm, SYBYL, MMP2 and AMPAC. Quanta 4.0 and CHARMm 22.2 (Molecular Simulations Inc., Burlington, MA), and SYBYL 5.22 (Tripos Associates, St. Louis, MO), and semiempirical molecular orbital calculations under AMPAC using the AM1 Hamiltonian (Quantum Chemistry Program Exchange, University of Indiana, Bloomington, IN) were employed on Silicon Graphics IRIS 4D/70GT or Indigo Elan 4000 systems (Mountain View, CA). MMP2 (Quantum Chemistry Program Exchange, University of Indiana, Bloomington, IN) calculations were performed on a microcomputer. X-ray crystal structures were retrieved from the Cambridge Structural Database and displayed using ALCHEMY III (Tripos Associates).

### Protein/Ligand NMR Studies

All NMR measurements were made on Bruker AM600 or AM500 spectrometers operating at 600.13 and 499.84 MHz for proton measurements and 150.92 and 125.68 MHz for carbon measurements respectively. All spectrometers were equipped with the Aspect 3000 data system and off-line data processing was performed using FELIX 2.1 or 2.3 (BIOSYM Technologies, San Diego, CA).

Samples containing 1 mM [$^{13}C_2$]-**5** or [$^{13}$C]-**6** and varying concentrations of β-LG (0–2 mM) were prepared in 10% $CD_3CD_2OD/D_2O$ (containing 75 mM NaCl/25 mM phosphate) adjusted to pD ~7.1. All spectra of these samples were collected at 308°K.

All 2D NMR experiments were conducted as variations of the HMQC experiment (24) in which the dipolar coupling (NOE), scalar coupling (COSY) or strong coupling (TOCSY) to the protons attached to the [$^{13}C_2$]-**5** or [$^{13}$C]-**6** labeled carbon atoms were allowed to build up after the HMQC magnetization transfer from $^{13}$C back to $^1$H. The $^{13}$C chemical shifts of [$^{13}C_2$]-**5** were determined in separate experiments so that the $t_1$ dimension ($^{13}$C) of the HMQC experiment could be restricted to 12–24 ppm ranges around one of the labeled carbon atoms. A representative schematic pulse sequence for the HMQC-NOE experiment would be: 90($^1$H)-1/2($J_{CH}$)-90($^{13}$C)-$t_{1/2}$-180($^1$H)-$t_{1/2}$-90($^{13}$C)-1/2($J_{CH}$)-90($^1$H)-1/2($J_{CH}$)-90($^1$H)-$t_m$-90($^1$H)-acquire ($t_2$ with GARP decoupling of $^{13}$C). Heteronuclear decoupling during data acquisition was accomplished by means of a GARP sequence.

The HMQC-NOE experiments (AM600) employed a $^1$H sweep width of 8929 Hz, and spectra were recorded with mixing times of 50–600 ms with the 1/2$J_{CH}$ delay tuned to the desired vinyl carbon-proton or methyl carbon-proton coupling constants (160 and 127 Hz respectively) appropriate for the experiment. The HMQC-COSY experiment was performed with the same $^1$H sweep width, but because of signal decay, the 1/4$J_{HH}$ delay was set to 5.5 ms instead of the optimal 13 ms to detect vinyl proton coupling. The HMQC-TOCSY experiments (AM500) were performed with a 7463 Hz $^1$H sweep width, a DIPSI-2 spin-lock sequence and spin-lock mixing times of 17-105 ms.

For these experiments in general, 96-320 scans of 4096 data points were collected in the $t_2$ dimension with a 1 s relaxation delay before each scan. In the $t_1$ dimension, 64 experiments were usually used with 2–4 dummy scans between experiments. The $t_2$ data were generally zero-filled once and apodized with a π/2 phase-shifted sinebell square function while $t_1$ data were generally subjected to 2 levels of zero-fill and apodized with a π/2 phase-shifted sinebell function.

## RESULTS

### Ligand NMR Studies

The $^1$H NMR spectra of **1**, **4**, and **7** were measured at 270 MHz and assigned as previously described (25). In earlier studies of ring-side chain orientations in **3** and **4** (8), Honig and co-workers utilized homoallylic coupling constants measured on a 100 MHz spectrometer to estimate ring-side chain dihedral angles. Here, the long range coupling constants were measured in $CDCl_3$ solutions at 500 MHz between the analogous homoallylic H-7 and H-4 and H-7 and 5-$CH_3$ protons in **1** and **4**. The J-values determined ($J_{H_{4,7}}$ = 1.80 Hz; $J_{H_{5,7}}$ = 0.91 Hz) are similar to those earlier observed for **4** by Honig and co-workers, and by fitting these values to their empirical equations (8) [$J_{H_{5,7}} \cong 1/2 \sin^2\theta$; $J_{H_{4,7}} \cong 0.3 + 3A/4 \sin^2\theta$, where A = 5-8 Hz], we predict a similar ring-side chain dihedral angle of 34–35° ± 5°. As originally pointed out by Karplus (8), this calculation cannot distinguish between these predicted twisted s-*cis* conformations about C5-C6-C7-C8 and their s-*trans* counterparts with ring-side chain torsion angles of about 150–160°, although NOE data shown below makes the predominance of an s-*trans* conformer unlikely.

Nuclear Overhauser enhancements, which arise due to relaxation of a nucleus by a magnetic dipole which is usually other nuclei within the molecule, are dependent on the internuclear distance between the dipoles and can thus provide information about molecular conformation. The $^1$H-$^1$H NOE's resulting from irradiation of the 1, 1′-, 5-, and 9-$CH_3$ groups were measured and the significant results for the H-7 and H-8 resonances for **1**, **4**, and **7** (and the H-11 resonance for **1**) are presented in Table 1. It should be noted that the geminal methyl groups at position 1 are chemical shift equivalent even at −130°C (ethanol-$d_6$), hence the single entries in Table 1 for NOE's upon irradiation of the 1,1′-$(CH_3)_2$ group.

For moderately flexible low molecular weight molecules like **1**, **4**, and **7** and in the absence of a known reference distance for the NOE's in Table 1, it is difficult to apply empirical treatments to estimate the retinoid ring-side chain dihedral angle. Nonetheless, the strong interaction between the 1, 1′-$CH_3$ and H-7 as well as the 5-$CH_3$ and H-8 makes a sole s-*trans* conformation unlikely. Qualitatively, the relative steady-state NOE also does not appear to differ dramatically whether the compounds are studied in solution in nonpolar solvents ($CDCl_3$) or in polar, protic media ($CD_3OD$ or buffer).

**Table I.** Nuclear Overhauser Enhancements for Retinoic Acid and β-Ionone

| Group irradiated | Compound | Solvent | Observed enhancement (%) H-7 | H-8 | H-11 |
|---|---|---|---|---|---|
| 1,1'-$(CH_3)_2$ | 1 | $CDCl_3$ | 12.0 | 6.0 | —[a] |
| | 1 | $CD_3OD$ | 8.7 | 1.6 | — |
| | 4 | $CDCl_3$ | 14.0 | 10.0 | [b] |
| | 4 | $CD_3OD$ | 14.0 | 8.0 | [b] |
| | 4 | buffer[c] | 11.6 | 8.5 | [b] |
| | 7 | $CD_3OD$ | 5.3 | 1.8 | [b] |
| 5-$CH_3$ | 1 | $CDCl_3$ | 2.6 | 3.8 | — |
| | 1 | $CD_3OD$ | 2.1 | [d] | — |
| | 4 | $CDCl_3$ | 4.6 | 7.2 | [b] |
| | 4 | $CD_3OD$ | 4.8 | 5.1 | [b] |
| | 4 | Buffer | 4.9 | 5.2 | [b] |
| | 7 | $CD_3OD$ | 1.0 | 2.3 | [b] |
| 9-$CH_3$ | 1 | $CDCl_3$ | 9.1 | [d] | [b] |
| | 1 | $CD_3OD$ | 12.8 | [d] | 8.7 |
| | 4 | $CDCl_3$ | 9.0 | 5.1 | 12.0 |
| | 4 | $CD_3OD$ | 11.2 | 7.3 | [b] |
| | 4 | Buffer | 10.5 | 5.6 | [b] |
| | 7 | $CD_3OD$ | 3.3 | 1.8 | [b] |

[a] No enhancement; observed enhancements are ±0.1–0.1%.
[b] Corresponding proton not present in structure.
[c] Buffer = 10% $CD_3CD_2OD/D_2O$ (with 75 mM NaCl, 25 mM phosphate; pD~7.1).
[d] Coupling effects prevented accurate integration.

## Ligand Modeling Studies

For computer modelling studies, **1**, **4**, and **7** were constructed initially with a planar side chain conformation and an s-*cis* ring-side chain relationship and then permitted to relax to a calculated minimum energy conformation. These starting structures were chosen because the data derived from our NMR and UV spectroscopy studies (not shown), as well as the X-ray crystal structure of the common triclinic form of **1** (26), suggest a preference for a planar, conjugated side chain both in the solid state and in solution.

Conjugate gradient minimization of **1**, **4**, and **7** using CHARMm led to predicted ring-side chain dihedral angles of 43°, 38°, and 43.5°, respectively (Table II). Other computational tools (MMP2, SYBYL, and AMPAC) predict similar preferred conformations for this torsion angle for **1**.

To assess the relative stability of the calculated minimum energy conformation with respect to the ring-side chain torsion angle, a grid conformational search about this torsion in **4** was performed in CHARMm. For this search, the torsion angle was incremented in 10° fixed steps; the remainder of the molecule was relaxed after each increment; and the CHARMm energy was recalculated. This strategy of relaxation after fixing each torsion angle increment, with the starting point for each minimization taken to be the calculated minimum energy conformation, has been suggested to lead to realistic relative energy predictions (27). Shown in Fig. 3 is the predicted relative energy versus torsion angle, where positive angles represent motion of the H-7 proton toward the reader (see Fig. 1). This profile is virtually identical to ones we found for **1** incremented in 5° fixed steps using either CHARMm or SYBYL (data not shown). All simulations yield as the lowest energy a slightly twisted 6-s-*cis* conformation (38°) although a twisted 6-s-*trans* conformation (H-7 moving away from reader) is also accessible (−28° and −80°to−110°).

**Table II.** Predicted Minimum Energy Ring-Side Chain Torsion Angles for **1**, **4**, and **7**

| Compound | Predicted optimized torsion (degrees) CHARMm | MMP2 | SYBYL | AMPAC |
|---|---|---|---|---|
| **1** | 43 | 31 | 37 | 47 |
| **4** | 38 | —[a] | 47 | — |
| **7** | 43 | — | 49 | — |

[a] Not performed.

## Protein/Ligand NMR Studies

It has been shown previously that when exposed to buffers containing ethanol, the secondary structure of β-LG begins a transition from predominantly β-strand to α-helix at about 20% ethanol by volume (28). Thus, a saturated solution of **4** in buffer containing only 10% ethanol was prepared, and the concentration of **4** in the supernatant was found to exceed the target concentration for NMR studies (1 mM) as assessed by UV spectrophotometry. However, the $^1H$ NMR spectrum of a 1 mM solution of **4** in deuterated ethanol/buffer exhibited a second set of broadened signals. That this was due to the presence of a micellar form of **4** in exchange with free ligand in solution was suggested by the finding that this second set of signals dissappeared upon dilution of this buffer with additional ethanol-$d_6$ and that ligand extraction from the buffer with $CHCl_3$ recovered **4** with its usual $^1H$ NMR spectrum in $CDCl_3$. Furthermore, titration of 1 mM **5** in 10% deuterated ethanol/buffer with increasing concentrations of β-LG (0, 0.1, 0.3, 1.0, and 2.0 mM) produced a progressive decrease in the second set of signals, which disappeared from both the $^1H$ and $^{13}C$ NMR spectra at 1–2 mM β-LG. Concomitantly, with increasing number of equivalents of β-LG, there is a progressive downfield chemical shift and broadening of the $^{13}C$ signals for **5** and an upfield shift and broadening of the vinyl proton resonances for **5**. This effect is maximal at 1–2 equivalents of β-LG and is consistent with both loss of the micellar form of **5** and its binding to β-LG.

With a β-LG bound solution of **5**, the HMQC-NOE experiment, which investigates NOE's from $^{13}C$-bound protons to other spatially near protons, was performed with the $^{13}C$ excitation frequency windowed around the labeled methyl group carbon (ca. 26.5 ppm) and a 150 ms mixing time. The results, seen in Fig. 4, show an NOE from the $^{13}C$-bound protons (2.19 ppm) to a prominent resonance at 7.2 ppm as well as a variety of signals from 0.5–2 ppm. Whereas the upfield observed signals likely represent intermolecular NOE's to aliphatic amino acid side chain groups on β-LG in close contact with **5**, the resonance at 7.2 ppm, which is close in chemical shift to that of the vinyl proton H-7 in unbound **5**, probably results from an intramolecular exchange mediated NOE. Performing the HMQC-COSY, with the $^{13}C$ excitation frequency set to that of the labeled vinyl carbon atom (ca. 130.6 ppm), since its attached proton is only coupled to the H-7 vinyl proton, helped establish

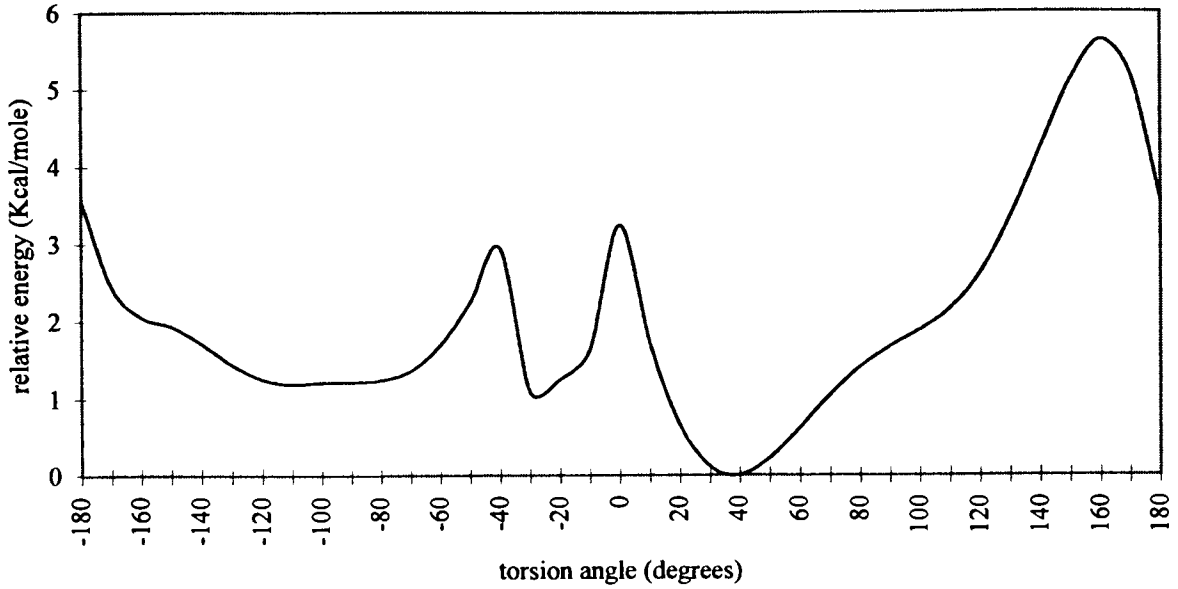


**Fig. 3.** The CHARMm energy versus ring-side chain torsion in **4** calculated as described in Materials and Methods.

that this resonance at 7.2 ppm in Fig. 4 is the H-7 vinyl proton of **5** (data not shown but available from author).

A second HMQC-NOE experiment was conducted with the $^{13}C$ excitation window set to that of the labeled vinyl carbon. As shown in Figure 5, an NOE was observed from the $^{13}C$ attached vinyl proton (ca. 6.2 ppm) to a resonance at ca. 1.7 ppm as well as to upfield signals, particularly at about 0.8 ppm. It seemed likely that the resonance at 1.7 ppm could be the protons of the methyl group on position 5 of ligand **5**, although it is slightly upfield of the resonance position for these protons in unbound **5**. Because of the long range coupling from the vinyl proton H-7 to the methylene protons at C-4 and the methyl protons on C-5 of **4**, the HMQC-TOCSY experiment was implemented with $^{13}C$ excitation of the vinyl carbon C-8 in hopes of seeing TOCSY transfer through H-7 to H-4 and the 5-$CH_3$ group. Unfortunately, no TOCSY transfer was observed beyond H-7 and the resulting spectrum was identical to that of of the HMQC-COSY experiment. A selective TOCSY experiment on **4** in $CDCl_3$, however did show the transfer (data not shown). The NOE observed at 0.8 ppm in Fig. 5 might also be to one or both of the geminal methyl groups on the 1-position of **5**, even though these methyl groups co-resonate downfield (ca. 1 ppm) in unbound **5**. Measurement of NOE mixing time build-up curves suggested that this NOE to a resonance at 0.8 ppm is dominated by spin diffusion. As shown in Fig. 6, with increasing mixing time the volume of the "cross peak" at 1.7 ppm divided by the "diagonal peak" at 6.2 ppm shows the expected linear increase at early mixing times, never exceeds the theoretical maximum ratio of 1, and is unobservable at long mixing times (i.e., 600 ms). On the other hand, the cross peak/diagonal peak ratio for the 0.8/6.2 ppm pair shows a parabolic increase, which substantially exceeds a ratio of 1 at longer mixing times, suggesting the dominance of spin diffusion (29). Spin diffusion is a phenomenon in which the rate of transfer of spin energy between nuclei becomes much larger than the rate of transfer of energy to the lattice and is frequently observed in NMR experiments involving macromolecules. It has been found that under such conditions the magnitude of

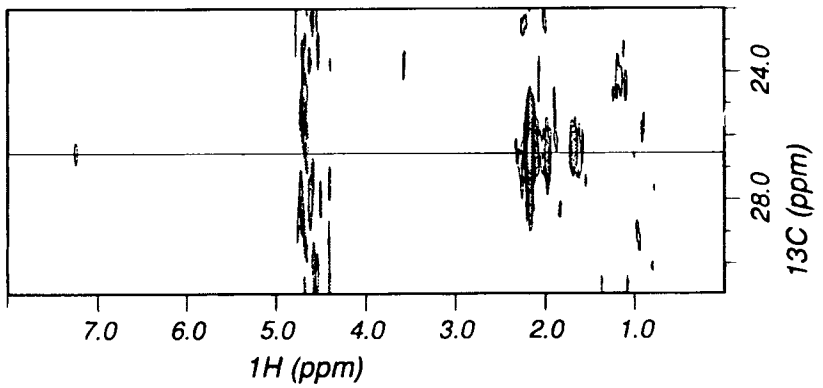


**Fig. 4.** The HMQC-NOE experiment results after irradiation of the labeled methyl carbon of **6** (ca. 26.5 ppm) and a 150 ms mixing time.

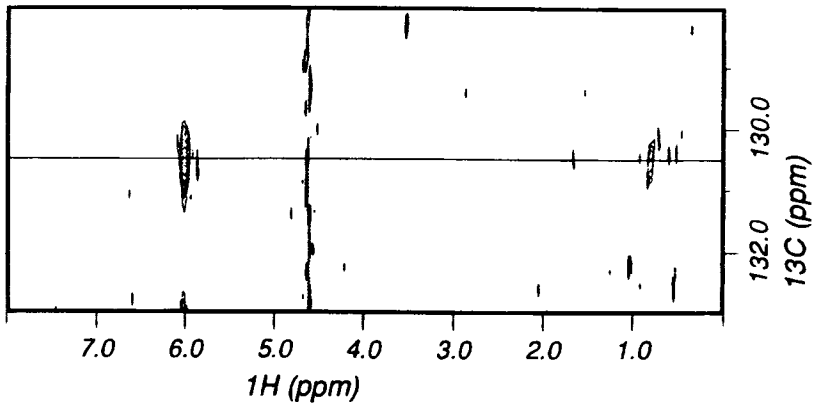


**Fig. 5.** The HMQC-NOE experiment results with **6**, performed as for Figure 4, except that the labeled vinyl carbon frequency was excited.

the NOEs observed does not have a simple relationship with the internuclear distance and may lead to relayed NOEs. Therefore the observed NOEs in these cases do not give much information about the conformation of molecules.

In an effort to confirm whether the NOE at 1.7 ppm in Fig. 5 is to the 5-$CH_3$ group of **5**, we prepared the alternative [5-$^{13}CH_3$]-β-ionone (**6**) as described above. Repetition of the HMQC-NOE ($t_m$ = 25–400 ms) experiment with β-LG bound **6** ($^{13}C$ at 22.6 ppm) shows significant NOE to aliphatic type resonances in the range of 0.8–1.9 ppm but nothing measurable to a resonance at 6.2 ppm (data not shown). This experiment with β-LG bound **6** does, however, show a resonance at the appropriate frequency of 1.7 ppm. That is, in β-LG bound **6** the protons bound to the labeled 5-$CH_3$ carbon resonate at the frequency that matches the frequency to which an NOE is observed when the H-8 proton is investigated in labeled **5**. As seen in Fig. 5, this suggests that there is dipolar relaxation of the H-8 vinyl proton by the 5-$CH_3$ in β-LG bound **5** seen in Fig. 5 and discussed below.

## DISCUSSION

As found by others for some of these retinoids, our measured long range coupling constants from H-7 to the 4-$CH_2$ and 5-$CH_3$ groups in **1** and **4**, as well as steady state NOE's observed to the vinyl protons in these molecules upon irradiation of the methyl groups, are consistent with these molecules assuming a preferred twisted 6-s-*cis* ring-side chain relationship when dissolved in chloroform, methanol or the buffer in which the β-LG bound ligand experiments were performed. The 4-oxo analog **7** was also subjected to measurement of steady state NOE's because, although modelling studies of **7** predicted a preferred conformation similar to **1** and **4**, the dipolar relaxation via the 4-$CH_2$ group upon irradiation of the 5-$CH_3$ group in **4** and **1** is substantial (~10–15% enhancement) and may be contributing to their observed small H-8/H-7% NOE ratios. As shown in Table I, while the magnitude of the steady state NOEs in $CD_3OD$ differ, the H-8/H-7 enhancement ratio for **7** is much greater than for **4** and is consistent with a somewhat twisted preferred ring-side chain conformation.

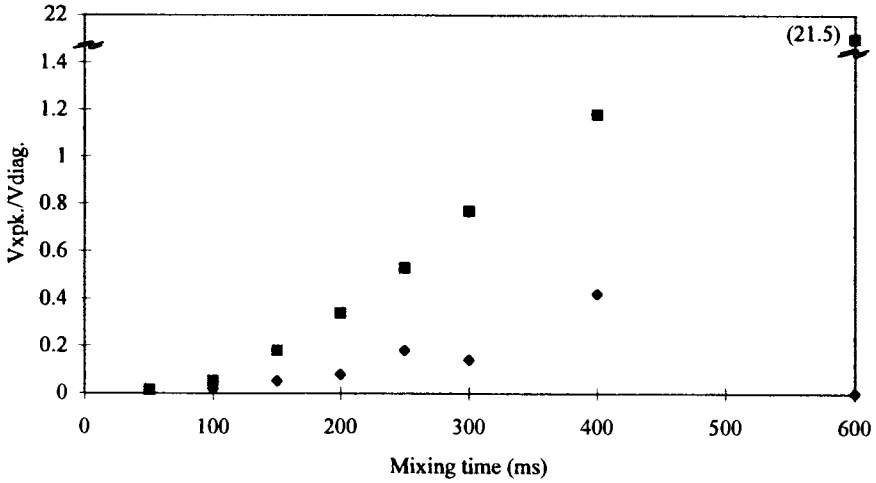


**Fig. 6.** NOE mixing time buildup curves expressed as volume of the cross peak (Vxpk.) divided by the volume of the diagonal peak (Vdiag.) for crosspeaks observed at 1.7 ppm (◆) and 0.8 ppm (■), as in Figure 4, with varying $t_m$.

Because of the moderate flexibility of these retinoids and the lack of an exact known reference distance in the compounds, it is difficult to use these NMR measurements to make certain estimates of the preferred ring-side chain torsion angle for the compounds in solution. However, the supposition that a somewhat twisted 6-s-*cis* relationship is preferred is supported by the calculations we and others (8,9) have performed. As seen in Table II, all of the computational methods employed predict a preferred ring-side chain torsion angle of 30–40° for **1**, **4**, and **7**. These predictions are bolstered by extensive conformational searching about this torsion as well as semiempirical molecular orbital calculations using the AM1 force field (data not shown) and are consistent with the results of the solution NMR studies of the retinoids.

When $^{13}C_2$-labeled **5** was bound to β-LG, results of the HMQC-NOE (and HMQC-COSY) experiments (Fig. 4) strongly suggest the retinoid model binds with a planar side chain conformation like that drawn for **5** in Fig. 1. The HMQC-COSY experimental results establish that the only prominent NOE observed from the $^{13}C$-labeled $CH_3$ group in **5** that we can ascribe to a known resonance is an intramolecular one to the H-7 vinyl proton consistent with the proposed planar side chain conformation for β-LG bound **5**. For example, the upfield NOE in Fig. 4 (ca. 1.5 ppm) does not coresonate with the protons of the 5-$CH_3$ group observed in β-LG-bound **6**. The HMQC-NOE experiment used to selectively examine NOEs from the H-8 vinyl proton (Figure 5) shows two prominent signals which appear likely to be to the 5-$CH_3$ group, and at least one of the 1-$CH_3$ groups of bound **5** or protein side chain groups. However, examination of the NOE mixing time buildup curves (Fig. 6) for the NOEs to the signals at 0.8 and 1.7 ppm clearly show that NOE to the 0.8 ppm resonance is dominated by spin diffusion and it is difficult to extract from this signal any certain information about this NOE. In an attempt to establish whether the NOE to the resonance at 1.7 ppm is an intramolecular one to the 5-$CH_3$ group in bound **5**, the HMQC-TOCSY experiment was conducted in efforts to observe TOCSY transfer from H-8 via H-7 to the 4-$CH_2$ and 5-$CH_3$ groups in β-LG bound **4** because of the scalar coupling between these protons in **4** in $CDCl_3$ solution. Unfortunately, no TOCSY transfer was observed beyond H-7, which may reflect the fact that the bound conformation of **5** is such that these coupling constants have become vanishingly small (this would occur if a 6-*cis* conformation becomes less twisted upon binding) or, perhaps more likely, these very small couplings may be unobserved due to shortened relaxation times for bound **5**. Therefore, we synthesized 5-[$^{13}CH_3$]-**6** and repeated the HMQC-NOE experiment. No NOE to the resonance position of the H-8 proton (6.2 ppm) was observed, but instead significant NOE to aliphatic signals from 0.8–1.5 ppm were observed. It seems plausible that when cross-relaxation of the 5-$CH_3$ group is measured, that the primary pathways for relaxation are to the 4-$CH_2$ group (which was observed at long mixing times and which is eliminated in **7**) and aliphatic amino acid side chains of β-LG in close contact with bound **6**. The HMQC experiment on β-LG bound **6** does, at least, show a resonance at the appropriate frequency (1.7 ppm) to increase confidence that the NOE from the H-8 vinyl proton is to the 5-$CH_3$ group of β-LG bound β-ionone. While our current labeling pattern does not allow us to make a certain estimate of the ring-side chain torsion angle, taken together our NMR results suggest β-ionone binds to β-LG with a planar side chain that has a 6-s-*cis* relationship to the trimethylcyclohexene ring like that shown in Figure 1.

This observation of a β-LG bound retinoid in a 6-s-*cis* conformation further illustrates that while the retinoids bind to a number of non-nuclear receptor binding proteins that are remarkably similar in their overall architecture, the conformation in which these ligands bind to the different proteins is surprisingly diverse. In addition to the known 6-s-*trans* conformation of retinal (**3**) bound to the structurally unrelated opsin (5), a similar conformation is observed for retinol (**2**) bound to CRBP and CRBPII in x-ray studies. In contrast, both X-ray and NMR studies of retinoic acid (**1**) bound to CRABPI and CRABPII show retinoid bound with a relatively planar side chain with a 6-s-*cis* relationship to the β-ionylidene ring. Furthermore, as mentioned above, the manner in which these ligands bind in the hydrophobic β-barrel of the SRBP, CRBPs, and CRABPs varies with respect to whether the hydrophobic β-ionylidene ring binds at the base of this pocket with the polar end group projecting to the protein surface or *vice versa* (see ref. 10).

On the basis of earlier absorption spectroscopy (30), fluorescence (15), and X-ray studies (16) of β-LG-retinol complexes, Cho and co-workers (19) have suggested that the $Trp^{19}$ residue of β-LG is an important amino acid at the base of the hydrophobic pocket interacting with the β-ionylidene ring and that $Lys^{70}$ near the mouth of this pocket associates with the polar end group. We see no NOE in our studies that is attributable to an intermolecular interaction between $Trp^{19}$ and our labeled β-ionones. However, if the published model of Cho and coworkers is correct, it is likely that alternative $^{13}C$-labeling sites in **4** (and **2**) should be useful in permitting these NMR studies to provide support for the proposed site and orientation of retinol binding in addition to the conformational information gained in these present studies.

## ACKNOWLEDGMENTS

This study made use of the National Magnetic Resonance Facility at Madison, which is supported by NIH grant RR02301 from the Biomedical Research Technology Program, National Center for Research Resources. Equipment in the facility was purchased with funds from the University of Wisconsin, the NSF Biological Instrumentation Program (DMB-8415048), NIH Biomedical Research Technology Program (RR02301), NIH Shared Instrumentation Program (RR02781), and the U.S. Department of Agriculture. Financial support of R.W.C., Jr. in the form of a Pfeiffer Memorial Faculty Development Research Fellowship from the American Foundation for Pharmaceutical Education is gratefully acknowledged.

## REFERENCES

1. R. C. Moon, R. G. Mehta, and K. V. N. Rao. Retinoids and cancer in experimental animals. In M. B. Sporn, A. B. Roberts, and D. S. Goodman (eds.), *The Retinoids: Biology, Chemistry, and Medicine*, 2nd Ed, Raven Press, New York, 1994, pp. 573–595.
2. D. R. Soprano and W. S. Blaner. Plasma retinol-binding protein. In M. B. Sporn, A. B. Roberts, and D. S. Goodman (eds.), *The Retinoids: Biology, Chemistry, and Medicine*, 2nd Ed., Raven Press, New York, 1994, pp. 257–281.
3. D. E. Ong, M. E. Newcomer, and F. Chytil. Cellular retinoid-

binding proteins. In M. B. Sporn, A. B. Roberts, and D. S. Goodman (eds.), *The Retinoids: Biology, Chemistry, and Medicine*, 2nd Ed., Raven Press, New York, 1994, pp. 283–317.
4. D. K. Manglesdorf, K. Umesono, and R. M. Evans. The retinoid receptors. In M. B. Sporn, A. B. Roberts, and D. S. Goodman (eds.), *The Retinoids: Biology, Chemistry, and Medicine*, 2nd Ed., Raven Press, New York, 1994, pp. 319–349.
5. S. O. Smith, J. Courtin, E. van den Berg, C. Winkel, J. Lugtenburg, J. Herzfeld, and R. G. Griffin. Solid state $^{13}C$ NMR of the retinal chromophore in photointermediates of bacteriorhodopsin: characterization of two forms of M. *Biochemistry* **28**:237–243 (1989).
6. E. Li, S.-j. Qian, N. S. Winter, A. d'Avignon, M. S. Levin, and J. I. Gordon. Fluorine nuclear magnetic resonance analysis of the ligand-binding properties of two homologous rat cellular retinol-binding proteins expressed in *Escherichia coli*. *J. Biol. Chem.* **266**:3622–3629 (1991).
7. A. W. Norris, D. Rong, S. A. d'Avignon, M. Rosenberger, K. Tasaki, and E. Li. Nuclear magnetic resonance studies demonstrate differences in the interaction of retinoic acid with two highly homologous cellular retinoic acid binding proteins. *Biochemistry* **34**:15564–15573 (1995).
8. B. Honig, B. Hudson, B. D. Sykes, and M. Karplus. Ring orientation of β-ionone and retinals. *Proc. Natl. Acad. Sci. USA* **68**:1289–1293 (1971).
9. R. Rowan, III, A. Warshel, B. D. Sykes, and M. Karplus. Conformation of retinal isomers. *Biochemistry* **13**:970–980 (1974).
10. E. Li and A. W. Norris. Structure/function of cytoplasmic vitamin A-binding proteins. In W. J. Darby, H. P. Broquist, and R. E. Olson (eds.), *Annu. Rev. Nutr., Vol. 16*, Annual Reviews, Palo Alto, 1996, pp. 205–214.
11. S. G. Hambling, A. S. McAlpine, and L. Sawyer. β-Lactoglobulin. In P. F. Fox (ed.), *Advanced Dairy Chemistry, Vol. 1*, Elsevier, Amsterdam, 1992, pp. 141–190.
12. M. D. Perez, M. C. Diaz de Villegas, L. Sanchez, P. Aranda, J. M. Ena, and M. Calvo. Interaction of fatty acids with β-lactoglobulin and albumin from ruminant milk. *J. Biochem.*, **106**:1094–1097 (1989).
13. H. M. Said, D. E. Ong, and J. L. Shingleton. Intestinal uptake of retinol: enhancement by bovine milk β-lactoglobulin. *Am. J. Clin. Nutr.* **49**:690–694 (1989).
14. P. Puyol, M. D. Perez, J. M. Ena, and M. Calvo. Interaction of bovine β-lactoglobulin and other bovine and human whey proteins with retinol and fatty acids. *Agric. Biol. Chem.* **55**:2515–2520 (1991).
15. E. Dufour and T. Haertle. Binding affinities of β-ionone and related flavor compounds to β-lactoglobulin: effects of chemical modifications. *J. Agric. Food Chem.* **38**:1691–1695 (1990).
16. H. L. Monaco, G. Zanotti, P. Spadon, M. Bolognesi, L. Sawyer, and E. E. Eliopoulos. Crystal structure of the trigonal form of bovine β-lactoglobulin and of its complex with retinol at 2.5 Å resolution. *J. Mol. Biol.* **197**:695–706 (1987).
17. M. Narayan and L. J. Berliner. Fatty acids and retinoids bind independently and simultaneously to β-lactoglobulin. *Biochemistry* **36**:1906–1922 (1997).
18. W. Gu and J. W. Brady. Molecular dynamics simulations of the whey protein β-lactoglobulin. *Protein Engin.* **5**:17–27 (1992).
19. Y. Cho, C. A. Batt, and L. Sawyer. Probing the retinol-binding site of bovine β-lactoglobulin. *J. Biol. Chem.* **269**:1102–11107 (1994).
20. S. W. Fesik, J. R. Luly, J. W. Erickson, and C. Abad-Zapatero. Isotope-edited proton NMR study on the structure of a pepsin/inhibitor complex. *Biochemistry* **27**:8297–8301 (1998).
21. R. W. Curley, M. A. Blust, and K. A. Humphries. A simple synthesis of [1,3-$^{13}C_2$]4-(2,6,6-trimethylcyclohexen-1-yl)buten-2-one (β-ionone). *J. Labelled Comp. Radiopharm.* **29**:1331–1335 (1991).
22. R. W. Curley and D. L. Carson. Synthesis of the 4-oxygenated retinoid metabolites. *Drug Des. Delivery* **1**:219–224 (1987).
23. J. D. White, R. W. Skeean, and G. L. Trammell. Lewis acid and photochemically mediated cyclization of olefinic β-keto esters. *J. Org. Chem.* **50**:1939–1948 (1985).
24. A. Bax, R. H. Griffey, and B. L. Hawkins. Correlation of proton and nitrogen-15 chemical shifts by multiple quantum NMR. *J. Magn. Reson.* **55**:301–315 (1983).
25. R. W. Curley and J. W. Fowble. Assignment of 'H and $^{13}C$ NMR spectra of retinoic acid isomers observed at the long wavelength UV-induced photostationary state. *Mag. Reson. Chem.* **27**:707–709 (1989).
26. C. H. Stam. Crystal structure of a monoclinic modification and the refinement of a triclinic modification of vitamin A acid (retinoic acid). *Acta Crystallogr. Sect. B.* **28**:2936–2945 (1972).
27. U. Burkert and N. L. Allinger. Pitfalls in the use of the torsion angle driving method for the calculation of conformational interconversions. *J. Comp. Chem.* **3**:40–46 (1982).
28. E. Dufour, C. Genot, and T. Haertle. β-Lactoglobulin binding properties during its folding changes studied by fluorescence spectroscopy. *Biochim. Biophys. Acta* **1205**:105–112 (1994).
29. J. Fejzo, Z. Zolnai, S. Macura, and J. L. Markley. Quantitative evaluation of two-dimensional cross-relaxation NMR spectra of proteins. Interproton distances in turkey ovomucoid third domain. *J. Magn. Reson.* **88**:93–110 (1990).
30. J. Horwitz and J. Heller. Properties of the chromophore binding site of retinol-binding protein from human plasma. *J. Biol. Chem.* **249**:4712–4719 (1974).